Structure, Properties and Reactivity of the $Fe^{II}Fe^{III}$ and $Zn^{II}Fe^{III}$ Purple Acid Phosphatases

Mark B. Twitchett[a] and A. Geoffrey Sykes*[a]

Keywords: Metalloenzymes / Purple Acid Phosphatases / Phosphate Ester Hydrolysis / Dinuclear metal active sites

This microreview describes the structure, properties and mechanisms of the purple acid phosphatases (PAP). The enzyme is isolated from mammalian, plant and bacterial sources. X-ray structural information is now available for the enzyme from pig (uteroferrin), rat and kidney beans. Features of the mechanism are the concerted action of a labile M^{II} centre (Fe^{II} or Zn^{II}) alongside a more inert Fe^{III}. The latter is effective as a conjugate-base $FeOH^{2+}$, which initiates hydrolysis at the M^{II}-bound phosphate ester by a process involving OH^- replacement of OR^- at the P^V. Histidine residues near to the active site help bind the phosphate and are involved in the release of OR^-. Effects of replacement of the Fe^{II} by Mn^{II}, Co^{II}, Ni^{II}, Cu^{II} and Zn^{II}, and of Fe^{III} by Ga^{III},Al^{III} and In^{III} have been studied. The mechanistic role of the $Zn^{II}Zn^{II}$ combination in alkaline phosphatases, and other related dinuclear centres is also considered.

Introduction

Proteins having dinuclear iron centres are a well characterised category with wide-ranging biological functions.[1−3] They include ribonucleotide reductase,[4][5] methane monooxygenase,[6][7] as well as the O_2-transport/storage protein hemerythrin,[8] and Δ^9 desaturase.[9] In addition the mammalian $Fe^{II}Fe^{III}$ active site in purple acid phosphatase (PAP) is able to catalyse the hydrolysis of phosphate esters written here as $(RO)PO_3H^-$ (Equation 1) where R is an organic group.[1−3,10−13]

$$(RO)PO_3H^- + H_2O \rightarrow H_2PO_4^- + ROH \quad (1)$$

However, such phosphatase action is not restricted to dinuclear Fe centres, with plant phosphatases using the dinuclear $Zn^{II}Fe^{III}$ combination.[14] Also alkaline phosphatases have $Zn^{II}Zn^{II}$ active centres, and zinc has a prominent role in both phosphatase and phosphoryl-transfer reactions.[1] Interestingly in the case of many zinc enzymes, X-ray structures of reactant, intermediate and product states have provided a lead in determining the mechanism. How-

[a] Department of Chemistry, University of Newcastle, Newcastle upon Tyne, NE1 7RU, UK

Professor A. G. Sykes FRS has BSc., Ph.D., and DSc. degrees in chemistry from the University of Manchester where he researched under the supervision of Professor W.C.E. Higginson. After post-doctoral work in Princeton and Adelaide, he was appointed a Lecturer at the University of Leeds, became a Reader in 1970 and moved to the Chair of Inorganic Chemistry at the University of Newcastle upon Tyne in 1980. His research is primarily in kinetic/mechanistic studies on both inorganic and bioinorganic (metalloprotein) reactions, with purple acid phosphatases a relatively recent interest.

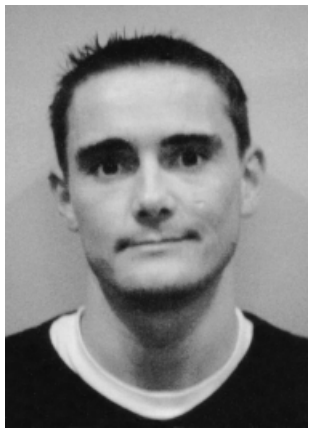

Mark Twitchett received his undergraduate education at the University of East Anglia and University of California Santa Barbara, obtaining his BSc. in Chemistry in 1992. He remained at the University of East Anglia for a further year to obtain his MSc in Spectroscopic and Physical Methods, and then researched with Professor A.G. Mauk on biological electron transfer at the University of British Columbia where he received his Ph.D. in Biochemistry and Molecular Biology in 1998. He has just completed a UK BBSRC Postdoctoral Research Assistantship with Professor Sykes in Newcastle.

MICROREVIEWS: This feature introduces the reader to the authors' research through a concise overview of the selected topic. Reference to important work from others in the field is also included.

  1434−1948/99/1212−2105 $ 17.50+.50/0

	Motif A						Motif B			
	*		* *		*		*		* *	
10	VAV**GDW**GGVPN	26	ILSL**GDN**F**Y**FTG	28	VL**AGNH**DHLG	84	V**AGH**Y**P**VW	26	YLC**GH**D**H**NLQ
9	VAV**GDW**GGVPN	26	VXSX**GDN**F**Y**FSX	28	XX**AGNH**DHXG	74	V**AGH**Y**P**VW	26	YXC**GH**D**H**NXQ
10	VAV**GDW**GGVPN	26	ILSL**GDN**F**Y**FTG	28	VL**AGNH**DHLG	84	V**AGH**Y**P**VW	26	YLC**GH**D**H**NLQ
131	GLI**GDL**GQSFD	17	VLFV**GDL**SYADR	26	WT**AGNH**EIEF	76	V**L**MH**SP**LY	28	VFA**GH**V**H**AYE
164	AVLN**DMG**YTNA	17	AWHG**GDL**SYADD	78	VLP**GNH**EASC	147	V**M**SH**RP**MY	26	YLS**GH**I**H**WYE

Figure 1. Sequence alignment of the purple acid phosphatases: Uteroferrin (Uf), beef spleen, human, kidney bean (*Phaseolus vulgaris*), and *Aspergillus ficuum*; conserved residues are indicated in bold and amino acids coordinating the dinuclear metal site are indicated by *[13]

ever, the intense colour stemming from the Fe^{III} component of mammalian and plant PAP′s has made possible kinetic/mechanistic studies using UV/Vis spectrophotometry.[15−18] Such studies are a major contribution to this review.

Function

Purple acid phosphates are nonspecific phosphomonoesterases which can be isolated from mammalian,[19−23] plant,[24−27] and microbial sources.[28][29] They are distinguished from other acid phosphatases by their purple colours. Mammalian PAP′s are highly conserved dinuclear metal-containing enzymes produced by the osteoclasts i.e. cells that reabsorb bone. The mammalian enzymes are distinguished from lysosomal and prostatic acid phosphatases by their resistance to inhibition by L(+)tartrate, and hence are known as tartrate-resistant acid phosphatases (TRAP′s).[30−32] In the osteoclast the enzyme is believed to be involved in dephosphorylation of phosphoproteins in the bone matrix, namely osteopontin and bone sialoprotein.[33] There have also been reports of low molecular weight phosphatase activity and removal of tyrosine-linked phosphates from the epidermal growth-factor receptor.[34] A role for PAP in the spleen involving degradation of aged red blood cells has also been proposed.[35] The degradation process may correlate to the generation of O_2-related free-radicals from redox changes at the Fe^{II} centre.[36] It has also been suggested that in Alzheimer patients there is a reduction in phosphatase activity in the brain due to a decrease in protein levels. In the case of plant PAP′s a physiological function appears to be the liberation of phosphate from organophosphates, which is important following phosphate starvation.[37]

Physical Properties of PAP

Purple acid phosphatases require acidic conditions for optimum activity and are characterised by an intense purple colour. The latter is brought about by a tyrosine phenolate to iron(III) ligand to metal charge-transfer (LMCT) process, which is observed for both the $Fe^{II}Fe^{III}$ and $Fe^{III}Fe^{III}$ states.[38−41] The PAP enzymes most extensively studied are those from the porcine uterus (known as uteroferrin, Uf, or pig PAP), bovine spleen (BSPAP), and from kidney beans (KBPAP). Complete amino acid sequences for a number of mammalian PAP′s are available (Uf,[42] bovine spleen,[42] human,[43] rat,[44] and mouse PAP.[45]) These have a dinuclear $Fe^{II}Fe^{III}$ active site ($M_r \approx 38$ kDa) and greater than 80% sequence homology. The plant PAP′s have less homology with only 60% identical residues for the enzymes from kidney bean (*Phaseolus vulgaris*) and *Arabidopis thaliana*,[46] and in the former the active site is known to be the $Zn^{II}Fe^{III}$ combination.[14]

Mammalian, plant, and bacterial sequences have revealed five regions of sequence homology which have been further grouped into two signature motifs (A and B)[47] (Figure 1). Thus despite differences in overall amino acid sequences, as well as molecular mass and subunit arrangement, the enzymes have structurally similar active site regions. The mammalian PAP active sites in Uf and BSPAP are spectroscopically well characterised. The dinuclear iron site can exist in two oxidation states, $Fe^{II}Fe^{III}$ (pink) and $Fe^{III}Fe^{III}$ (purple). Of these only the $Fe^{II}Fe^{III}$ combination peak at 515 nm ($\varepsilon = 4450 M^{-1}cm^{-1}$), has significant phosphatase activity.[48][49] The $Fe^{II}Fe^{II}$ state generated by dithionite (0.5 mM) reduction (30 min) has no long term stability, and has not been studied in a similar way. Loss of Fe^{II} occurs, and after 30 min only 40% recovery of the higher oxidation states is possible.[17] The purple $Fe^{III}Fe^{III}$ form is EPR silent and gives a characteristic UV/Vis peak at 550 nm ($\varepsilon = 4300 M^{-1}cm^{-1}$). Recently magnetic susceptibility measurements on protein in the $Fe^{II}Fe^{III}$ states have indicated exchange coupling constants, J values between -5 and $-15 cm^{-1}$ for KBPAP and BSPAP in both states,[50] with the main contribution to antiferromagnetic coupling from the μ-hydroxo bridge.[51][52] Analysis of iron K-edge EXAFS data has suggested that a μ-hydroxo or alkoxy group may be present.[53] Recent CD/MCD studies on this redox state provide confirmation of antiferromagnetic coupling and suggest a μ-hydroxo group.[54] The EPR spectrum of the $Fe^{II}Fe^{III}$ enzyme, with g values at 1.94, 1.76 and 1.56 is consistent with coupling between the high-spin Fe^{II} and Fe^{III} ions.[50,55,56]

In addition to the bridging hydroxo group the existence of a coordinated aqua/hydroxo group to each Fe has been demonstrated by ESEEM (electron spin echo envelope modulation),[57] ENDOR (electron nuclear double resonance),[58] and is consistent with electrochemical studies.[59] Furthermore the remaining endogenous ligands have been

identified by a variety of spectroscopic methods. The intense purple/pink absorbance at 500−600 nm is assigned to a tyrosine phenolate to Fe^{III} charge-transfer band.[60−63] The presence of the tyrosine accounts for the retention of one Fe in the +3 state. The $Fe^{III}Fe^{III}/Fe^{II}Fe^{III}$ reduction potential (E°) is 367mV vs. NHE, whereas that required for the further reduction of $Fe^{II}Fe^{III}$ is negative.[59] Tyrosine is also a ligand in transferrin, active-site coordination $[Fe(Tyr)_2(His)(Asp)(CO_3)]$, where E° for the Fe^{III}/Fe^{II} couple is −520mV,[64] a measure of the difficulty of bringing about the reduction of a tyrosine-coordinated Fe^{III}. Additional evidence from Resonance Raman and ^1H NMR spectroscopy confirms that a tyrosine is bound to the Fe^{III} in PAP.[60−63] Coordination of imidazole and of carboxylate groups have been confirmed by ^1H NMR spectroscopy.[61][62] Pulse EPR[65] and Mossbauer[51,66,67] studies have also been carried out. A demonstration that both Fe atoms are six coordinate comes from CD/MCD investigations,[54] and all information obtained is consistent with the active site structure indicated in Figure 2. It should be noted however that the ^1H NMR studies provide no evidence for a second His coordinated to the Fe^{II}. Fast exchange of the Nε proton with bulk solvent is a possible explanation of effects observed. Studies on plant KBPAP have also been carried out.[48] Acid dissociation pK_a′s for KBPAP determined by UV/Vis absorption spectrophotometry of 4.8 and 9.5 have been assigned to H_2O ligands to the Fe^{III} and Zn^{II} respectively.[11] For BSPAP the first pK_a is also at 4.8,[48] whereas for Uf a smaller value of 3.8 is found.[16]

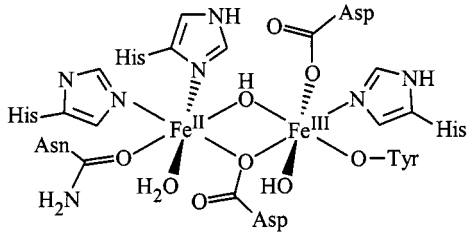

Figure 2. Structure of the $Fe^{II}Fe^{III}$ active sites of mammalian purple acid phosphatases

X-ray Structures

X-ray crystal structures of the 111 kDa homodimeric $Zn^{II}Fe^{III}$ KBPAP enzyme (resolution 2.65Å), the same protein with μ-phosphate coordinated (2.7Å), and the product with μ-tungstate(VI) inhibitor coordinated (3.0Å) have been reported.[11] More recently the structures of μ-phosphato derivatives of two mammalian PAP′s from Uf (1.55Å),[68] and from rat (2.7Å),[69] both believed to be in the $Fe^{III}Fe^{III}$ state, have been determined. The mammalian PAP enzymes are monomeric glycoproteins of ≈ 38 kDa, whereas the two monomer units of KBPAP are connected by a disulfide bridge. Sequence homologies between the monomer unit of the homodimeric KBPAP and mammalian PAP′s have been investigated.[47] With the *N*-terminal domain of KBPAP removed the two enzymes can be aligned. The C-terminal domain incorporates two sandwich βαβαβ motifs. All the ligands to the dimetal site are found within these two motifs.

The high resolution Uf structure confirms octahedral coordination at both metals.[68] The $Fe^{III}-Fe^{III}$ separation is 3.31Å and the phosphate bridges the two metals in a symmetrical manner. Strong electron density is observed consistent with the presence of a μ-hydroxo group, and there is no evidence for phosphate displacing this group. The two metals are also bridged in a monodentate manner by one of the aspartate residues, and there is confirmation that the tyrosine phenolate O-atom is bound to the Fe. The spacial arrangement of the metal ligands are very similar to those in KBPAP, and the α-carbon atoms of all seven coordinated amino acid residues superimpose. The active site is readily accessed from the surrounding solvent. The protein fold of Uf resembles that of KBPAP and some serine/threonine proton phosphatases, despite the <15% homologies.

The KBPAP structure has a $Zn^{II}Fe^{III}$ active site,[11] and unlike the $Fe^{III}Fe^{III}$ Uf and rat structures, is the only one for which the dimetal site is in the active form. The Zn^{II} is ligated to the Nε atom of His-286, the Nδ atom of His-323 and the carbonyl oxygen of Asn-201 (Figure 3). The Fe^{III} is ligated to the Nε atom of His-325, to Tyr-167 and the carboxylate of Asp-135. The Zn−Fe separation is 3.26Å. Three exogenous H_2O/OH^- ligands were modelled into the active site. These are a terminal hydroxo ligand to the Fe^{III}, a terminal H_2O to the Zn^{II}, and a μ-hydroxo bridge between the two metals. From sequence homologies and spectroscopic studies a high degree of conformity with the mammalian active site is indicated (Figures 2 and 3). The similarity of the dimetallic ligation with those of the serine/threonine protein phosphatases, calcineurin (PP2B) and PPI is noted.[70−73]

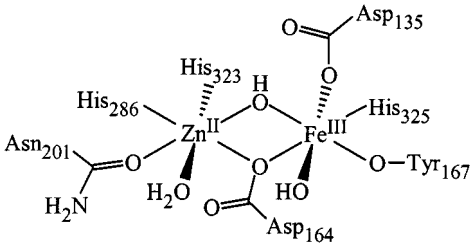

Figure 3. Structure of the $Zn^{II}Fe^{III}$ active site of kidney bean purple acid phosphatase (KBPAP) from X-ray crystallography[11]

In addition three histidine (His 202, 295 and 296) are located near to the dimetallic centre of KBPAP (Figure 4), and are in positions where they can interact with phosphate.[11] It has been proposed that the His-296 protonates the leaving alcohol group. The counterparts of these residues are His-92, Glu-194 and His-195 in the mammalian PAP′s.[68][69] In the two mammalian structures the His-92 and His-195 residues are hydrogen-bonded to the phosphate.[68] The side chain of Glu-194 is not in close contact with the phosphate, and appears to have no similar role to that of His-295 in KBPAP. The conservation of two of the

histidines (His-202 and 296), and their superposition in the different structures, suggests a mechanistic role.

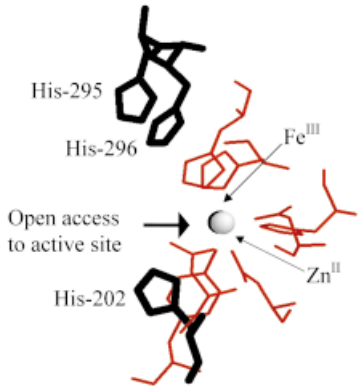

Figure 4. Structure of KBPAP illustrating the close proximity of residues His-202, -295 and -296 to the dinuclear metal active site

Structures of Other Phosphatases

The PAP′s are members of a much larger family of phosphatases recently reviewed.[1] Two other categories, the alkaline phosphatases (AP),[1][74] and the serine/theonine protein phosphatases (PP),[70−73] are mentioned here. The alkaline phosphatases are colourless and have a linear arrangement of two Zn^{II} atoms 4.1Å apart, and a Mg^{II} at 4.8Å. The structure of the native enzyme with phosphate bound (2.0Å resolution) has provided most information. The phosphate substrate bridges Zn1 and Zn2, which have no other bridging ligands, whereas Asp-51 bridges bidentately Zn2 to Mg3 (the third metal atom) (Figure 5).

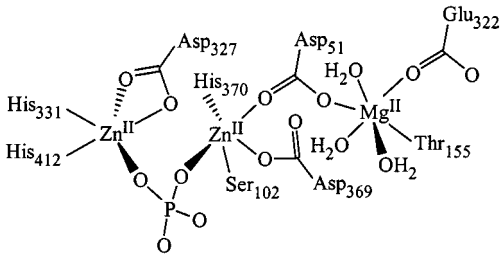

Figure 5. Structure of the $Zn^{II}Zn^{II}Mg^{II}$ active site of alkaline phosphatase with phosphate bound[1]

The Zn1 centre is pentacoordinated by bidentate Asp-327, His-331, His-412 and the O-atom of the phosphate group. The Zn2 is tetrahedral and coordinated by Asp-51, Asp-369, His-370 and phosphate. The Mg3 is ooctahedral with all O-donors, Asp-51, Thr-135, Glu-322 and three H_2O′s. The remaining two O-atoms of the phosphate are tightly held by hydrogen-bonds with the guanidinium group of Arg-166. A particular feature of the mechanism is the incorporation of $(RO)PO_3^{2-}$ into a serine phosphate-ester intermediate (Figure 6) which has been identified by X-ray crystallography.[1]

Coordination of the Ser-102 O-atom to the Zn2 facilitates deprotonation of the side chain, and the serinate nucleophile attacks the phosphate and replaces the OR^- group. The intermediate so formed reacts further with H_2O to give the hydrolysed product. AP appears unique amongst these enzymes in reacting by a two-stage mechanism. The Mg3 ion appears to have a minor role only.

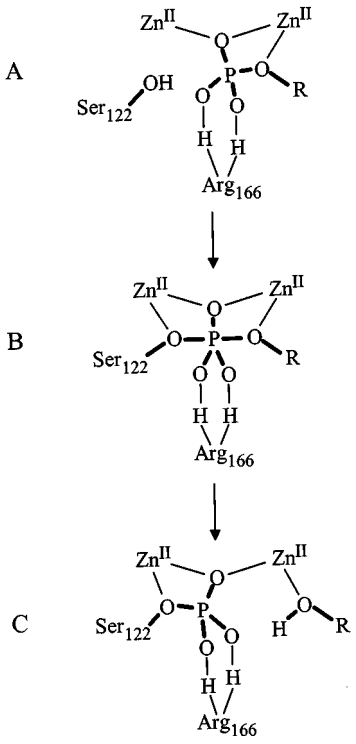

Figure 6. Schematic illustration of the conversion of $(RO)PO_3H^-$ (A) into a serine phosphate ester intermediate (C) by alkaline phosphatase

PP proteins are activated by several metal ions, and probably contain the Fe−Zn combination in the native form. The X-ray crystal structure of the phosphate bound rabbit muscle PP (PP-1) has been determined to 2.1Å resolution,[72] and the dinuclear metal site superimposes well with KBPAP, particularly with respect to the bridging ligands. The metals are both five-coordinate and are 3.3Å apart. They are bridged by an oxygen of Asp-92 and a water (very likely hydroxide). One metal has a distorted trigonal-bipyramidal geometry and additional coordination to Nε of His-173, Nδ of His-248 and the carbonyl oxygen of Asn-124. The other metal ion has a square-pyramidal geometry and additional coordination to Nε of His-66, Asp-64 and another solvent molecule (Figure 7). A notable difference is the substitution of a solvent H_2O for the tyrosine in PAP, and no purple colour is therefore observed.

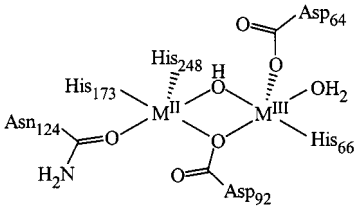

Figure 7. Structure of the active site of rabbit muscle protein phosphatase (PP-1)[72]

Activity of PAP

With the further elucidation of PAP active-site structures it is possible to consider in more detail the mechanism by which these proteins hydrolyse phosphate esters in acidic conditions. Such mechanistic studies have featured prominently in work carried out at Newcastle, with particular emphasis on kinetic analysis of UV/Vis spectrophotometric changes for the interaction of oxyanions with the enzyme.[16][18] Activity measurements are carried out by monitoring UV/Vis changes for the release of nitrophenol from *p*-nitrophenol phosphate, or α-naphthol from α-naphthyl phosphate. The initial slope of a plot of α-naphthol released against time gives the activity in nmol·min^{-1}. In previous studies unit enzyme activity was defined as the amount of enzyme catalysing the hydrolysis of 1 μmol of α-naphthyl phosphate per min. Following observations that the activity of BSPAP exhibits a bell-shaped pH dependence, Witzel and colleagues[48] proposed that two single proton equilibria were involved. One of these for the upward part of the bell-shape curve gives a pK_a of 4.8 and is catalytic, and the second for the downward part gives a pK_a of 6.9 which inhibits reaction. The lower pK_a is also observed in EPR and UV/Vis studies,[48] and has been attributed to deprotonation of the solvent H_2O coordinated to the Fe^{III}. Based on evidence that no nucleophilic residue on the enzyme appears to be involved in the catalytic reaction, and that no covalent bound intermediate is formed as in the case of the phosphotransferases, it has been concluded that a hydroxo ligand bound to the Fe^{III} induces the ester hydrolysis reaction.[16][48] Results obtained from the reaction of labelled adenosine 5′-triphosphate (ATP) with $Fe^{II}Fe^{III}$ PAP have demonstrated that there is transfer of phosphate to an H_2O position on the PAP with overall inversion at the phosphate.[75]

Reaction of Phosphate ($H_2PO_4^-$) With Uf PAP

Although reactions of the $Fe^{II}Fe^{III}$ protein with a number of oxyanions had been studied quite extensively,[19,51,54,61,65,76,77] there has until recently been no clear understanding of the precise function of the Fe^{II} and Fe^{III} combination. At 25°C acid dissociation pK_a values for H_3PO_4 are 2.1 for the formation of $H_2PO_4^-$, and 6.7−7.0 for the formation of HPO_4^{2-}. On addition of excess of phosphate ($H_2PO_4^-$) to $Fe^{II}Fe^{III}$ rapid stopped-flow formation of a phosphato product is observed. Spectrophotometric changes gave a shift in UV/Vis peaks from 515 nm for $Fe^{II}Fe^{III}$ to 535−560 nm (pH dependent) for the phosphato product. Surprisingly first-order rate constants k_{obs} obtained by monitoring absorbance changes at 620 nm indicate that the reaction is independent of $[H_2PO_4^-]$ in the range 10−50 mM (Figure 8).[16] The reactions with phenyl phosphate, pyrophosphate, tripolyphosphate and ATP (adenosine 5′-triphosphate), referred to collectively as PO_4, in which ester hydrolysis occurs, are also independent of $[PO_4]$.[16] Significantly, with $(MeO)_3PO$ no absorbance changes are observed indicating the need for two strongly nucleophilic oxo groups (and/or hydrophilic groups) for attachment to the Fe^{III} chromophore to occur. The latter does however inhibit the reaction of $H_2PO_4^-$, suggesting that an interaction of $(MeO)_3PO$ with Fe^{II} is occurring.

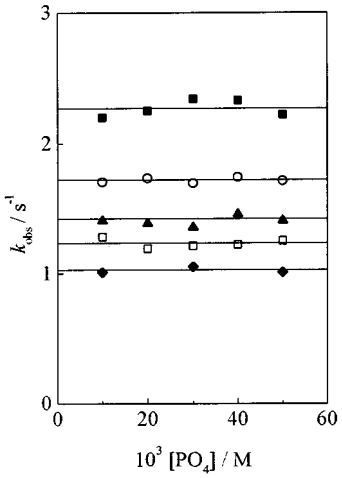

Figure 8. The phosphate concentration independence of first-order rate constants k_{obs} (25°) for the reaction of $Fe^{II}Fe^{III}$ Uf with different phosphates: $H_2PO_4^-$ (○), phenyl phosphate (□), pyrophosphate (■), tripolyphosphate (▲) and ATP (◆) at pH 4.6, I = 0.01M (NaCl)[16]

The mechanism proposed in the case of $H_2PO_4^-$ involves binding first to the Fe^{II}, in a relatively rapid process which does not contribute appreciably to changes in visible absorbance. Bridging to the strongly chromophoric Fe^{III} then occurs. Such a mechanism is consistent with general properties of high-spin Fe^{II} and Fe^{III} ions, the hexaaqua ions of which have water-exchange rate constants close to $10^6 s^{-1}$, and $10^3-10^4 s^{-1}$, respectively.[78][79] Accordingly the reaction sequence can be expressed as in Equation (2).

$$PO_4 + M^{II}\ldots Fe^{III} \underset{}{\overset{K_1.}{\rightleftharpoons}} M^{II}\ Fe^{III} \quad (2)$$
$$\quad\ |\ \ | \qquad\qquad\quad |\ \ |$$
$$\quad H_2O\ OH \qquad\qquad PO_4\ OH$$

followed by bridging to the strongly chromophoric Fe^{III}, (3).

$$M^{II}\ldots Fe^{III} \underset{k_b}{\overset{k_f}{\rightleftharpoons}} M^{II}\ldots Fe^{III} \quad (3)$$
$$|\ \ \ | \qquad\qquad\quad \backslash\ \ / \qquad\qquad$$
$$PO_4\ OH \qquad\qquad\quad PO_4$$

Assuming (2) to be relatively rapid, mass balance can be used to give (4)

$$k_{obs} = \frac{k_f K_1 [PO_4]}{K_1 [PO_4] + 1} + k_b \quad (4)$$

However the first term on the right-hand side suggests that a $[PO_4]$ dependence should be observed. Only if k_b is

dominant, or $K[PO_4] >> 1$ is this equation consistent with the observed $[PO_4]$ independence. There is no evidence for k_b being dominant, and the second possibility is therefore considered. Determination of the overall stability constant K by titration of Uf PAP with $H_2PO_4^-$ at pH 4.9 (40 mM acetate) gives a value of $165M^{-1}$,[80] in agreement with an earlier value of $151M^{-1}$ in 100 mM acetate buffer.[80] No dependence of thermodynamic and kinetic parameters on acetate in the range 25−55 mM, has been observed.[15] The overall K can be written as $K_1\ k_f/k_b$, or K_1K_2 on replacing k_f/k_b with K_2. For the 10−50 mM range of $[PO_4]$ studied no dependence on $[PO_4]$ is observed, and it is concluded that $K_1[PO_4] >> 1$, or alternatively $K_1[PO_4]$ is say > 5, which gives $K_1 > 500\ M^{-1}$. Since K has been determined as $165M^{-1}$, K_2 for the intramolecular step (3) is <0.32. It should be noted that K and K_2 have different units, and that K_1 may benefit from association at the His residues previously indicated, e.g. Figure 8.

It is not clear how the HPO_4^{2-} bridge dissociates. There are two possibilities to consider: (a) by cleavage of the $Fe^{II}-PO_4$ bond, or (b) cleavage of $Fe^{III}-PO_4$. If the first of these applies then dissociation follows a different route to formation. Two of the residues His-202, His-295 and His-296 found in KBPAP are conserved as His-92 and His-195 in mammalian forms, and may help bind the $H_2PO_4^-$ in (2). The mechanism of ester hydrolysis is considered below after sections on the reactions with other oxyanions and redox studies.

Reactions With Other Oxyanions

Further insight into the mechanism of oxyanion binding has been provided by studies on the binding of arsenate(V), molybdate(VI) and tungstate(VI) to $Fe^{II}Fe^{III}$ Uf.[18] Both phosphate and arsenate function as weak competitive inhibitors for phosphate ester hydrolysis by acting as bridging ligands between the two metal centres.[16,19,53,80−83] These oxoanions lower the protein reduction potential and increase the susceptibility of the active site to air oxidation.[58][59] Conversely, tungstate(VI) and molybdate(VI) are reported to be strong noncompetitive inhibitors which increase the reduction potential and stabilise the active site.[18,57,59] It has been suggested that the latter two oxoanions bind in a different manner to the phosphate and arsenate(V), producing a change in the active site EPR spectrum from rhombic to axial, and a change in the UV/Vis spectrum (molybdate). A low resolution structure is available for tungstate(VI) bound to KBPAP.[11] Recent CD/MCD studies on protein having bound phosphate or molybdate have led to the proposal that bound phosphate, unlike molybdate, interacts with the active site μ-OH bridge thus increasing the bond strength between the μ-OH bridge and the Fe^{II}, and producing a more rhombic Fe^{II} centre.[54] EXAFS results have also been reported on $Zn^{II}Fe^{III}$ Uf.[77] A number of anomalies remain, and further work is required in this area.

As far as the kinetics of the reactions of $Fe^{II}Fe^{III}$ Uf with oxyanions XO_4 (molybdate, tungstate and vanadate) are concerned, rate laws independent of $[XO_4]$ are similar to those obtained with $H_2PO_4^-$ phosphate.[18]

Redox Studies on Uf PAP

Two inorganic reagents, $[Fe(CN)_6]^{3-}$ (E° = 410mV) and $[Co(phen)_3]^{3+}$ (E° = 370mV) have been used as oxidants (25°C) for $Fe^{II}Fe^{III}$ Uf PAP, at pH 5.0, I = 0.10M (NaCl), overall Equations (5) and (6).[17]

$$Fe^{II}Fe^{III} + [Co(phen)_3]^{3+} \rightarrow Fe^{III}Fe^{III} + [Co(phen)_3]^{2+} \quad (5)$$

$$Fe^{II}Fe^{III} + [Fe(CN)_6]^{3-} \rightarrow Fe^{III}Fe^{III} + [Fe(CN)_6]^{4-} \quad (6)$$

With $[Co(phen)_3]^{3+}$ as oxidant first-order dependencies on both reactants are observed, giving second-order rate constants k_{Co} of $1.26M^{-1}s^{-1}$. In contrast the reaction with $[Fe(CN)_6]^{3-}$ gives saturation kinetics (Figure 9). This behaviour can be explained by the reaction sequences (7) and (8).

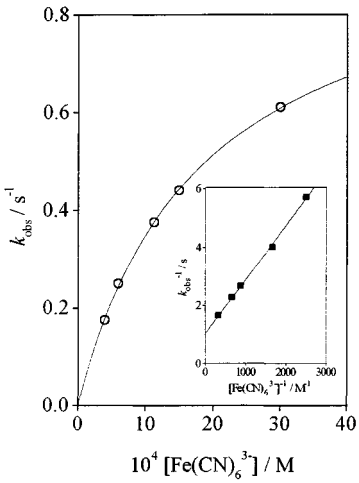

Figure 9. Saturation kinetic behaviour of first-order rate constants k_{obs} (25°C) for the reaction of $Fe^{II}Fe^{III}$ Uf with $[Fe(CN)_6]^{3-}$ at pH 5.0, I = 0.10M (NaCl). The inset shows the reciprocal plot[17]

$$Fe^{II}Fe^{III} + [Fe(CN)_6]^{3-} \overset{K_{Fe}}{\rightleftharpoons} Fe^{II}Fe^{III}\ldots[Fe(CN)_6]^{3-} \quad (7)$$

$$Fe^{II}Fe^{III}\ldots[Fe(CN)_6]^{3-} \overset{k_{Fe}}{\rightarrow} Fe^{III}Fe^{III} + [Fe(CN)_6]^{4-} \quad (8)$$

The part played in phosphate ester hydrolysis by the positive patch of His-202, His-295 and His-296 near to the active of KBPAP (Figure 4) has been discussed.[11] Two of these histidines, His-92 and His-195, are conserved in Uf. Association of $[Fe(CN)_6]^{3-}$ at this site (7), prior to electron transfer (8) is proposed therefore. For such a sequence (9) is derived,

$$k_{obs} = \frac{k_{Fe}\,K_{Fe}\,[Fe(CN)_6^{3-}]}{1 + K_{Fe}\,[Fe(CN)_6^{3-}]} \quad (9)$$

and a graph of $1/k_{obs}$ against $1/[Fe(CN)_6^{3-}]$ is linear. The slope and intercept give K_{Fe} and k_{Fe} values of $540M^{-1}$ and

$1.00s^{-1}$ respectively. Moreover competitive inhibition of the $[Fe(CN)_6]^{3-}$ oxidation by nonredox active $[Cr(CN)_6]^{3-}$ and $[Mo(CN)_8]^{4-}$ is also observed with association constants as defined in (7) of $K_{Cr} = 550M^{-1}$ and $K_{Mo} = 1580M^{-1}$. Together these studies provide support for an electrostatically controlled interaction. The magnitude of the association constants suggests an effective local protein charge as high as +4,[84] which could arise from two $HisH^+$ groups along with some contribution from the active site charge. We note that although the positively charged region on PAP favours anionic reagents, substrates which are cationic also retain an appreciable reactivity. Thus the reaction of $Fe^{III}Fe^{III}$ Uf PAP with the positively charged reductant $[Ru(NH_3)_5H_2O]^{2+}$ ($E° = 67mV$) (10),

$$Fe^{III}Fe^{III} + [Ru(NH_3)_5H_2O]^{2+} \rightarrow Fe^{II}Fe^{III} + [Ru(NH_3)_5H_2O]^{3+} \quad (10)$$

gives a second-order rate constant k_{Ru} of $2.2 \times 10^5 M^{-1}s^{-1}$. The magnitude of the rate constants k_{Co} and k_{Ru} suggest a dependence on thermodynamic driving force.

Effects of pH on PAP Reactivity

Rate constants for the reactions of $H_2PO_4^-$ and phosphate esters $(RO)PO_3H^-$ with $Fe^{II}Fe^{III}$ Uf are dependent on pH in the range 2.6−6.5 (Figure 10).[16]

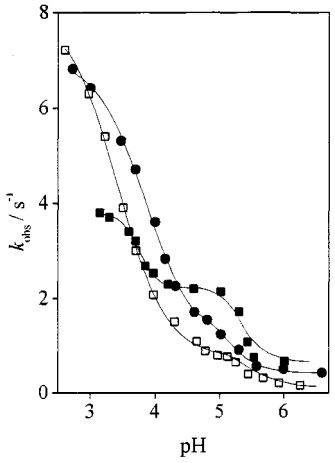

Figure 10. Variation of first-order rate constants k_{obs} (25°C) with pH for the reaction of $Fe^{II}Fe^{III}$ Uf with $H_2PO_4^-$ (●), phenyl phosphate (□), and pyrophosphate (■), $I = 0.10M$ (NaCl)[16]

Contributions to pH effects can stem from acid-base effects involving aqua ligands, nearby protein amino acids, and/or free and monodentate phosphate species. In the reaction of $H_2PO_4^-$ rate constants k_{obs} provide evidence for a Uf pK_{1a} of 3.9, which is assigned to acid dissociation at the Fe^{III}.[16] There is some evidence (the inflection at pH ≈ 5) for a second process pK_{2a}. In all other cases (phenyl phosphate, pyrophosphate, tripolyphosphate and ATP) two pK_a values (pK_{1a} and pK_{2a}) are clearly apparent, and rate constants k_1, k_2 and k_3 can be defined for the reactions of different protonated/deprotonated forms of the adduct formed in the first step of Scheme 1.

From the mechanism proposed the rate law (11) can be derived.

$$k_{obs} = k_1 + \frac{(k_3\text{-}k_1)\,K_{1a}K_{2a} + (k_2\text{-}k_1)\,K_{1a}[H^+]}{[H^+]^2 + K_{1a}[H^+] + K_{1a}K_{2a}} \quad (11)$$

From fits to (11) values of K_{1a}, K_{2a}, k_1, k_2 and k_3 are obtained (Table 1). The pK_{1a} values determined are in the range 3.4−3.9 (average 3.8), and are attributed to deprotonation of the Fe^{III} bound H_2O. The same pK_a is obtained from the effects of pH on the UV/Vis absorbance of Uf. As a guide the first acid dissociation constant of $[Fe(H_2O)_6]^{3+}$ is 3.0, whereas $[Fe(H_2O)_6]^{2+}$ remains in the aqua form until >7.[85] The second deprotonation effect (pK_{2a}) suggests that acid dissociation at the phosphate group attached to the Fe^{II} is contributing (Figure 10). As is to be expected shifts are observed in pK_{2a} values, as compared to literature values for the free phosphate reactant (which are 0.4−0.7 pH units higher), as a result of complexing to Fe^{II} and changes in the immediate environment. In the case of $H_2PO_4^-$ this would require that the pK_a of 6.7−7.0 is shifted to 5.1 on attachment to Fe^{II}. For a full treatment the further effect of deprotonation of nearby His residues also needs to be considered.

The effects of pH on activity have been studied to higher pH′s with α-naphthyl phosphate, as illustrated in Figure 11. Maximum activity for Uf is observed at pH 4.9 whereas in the case of KBPAP and BSPAP a shift to the range pH ≈ 5.9 is observed. Earlier studies on Uf with *p*-nitrophenyl phosphate have also indicated maximum activity at pH

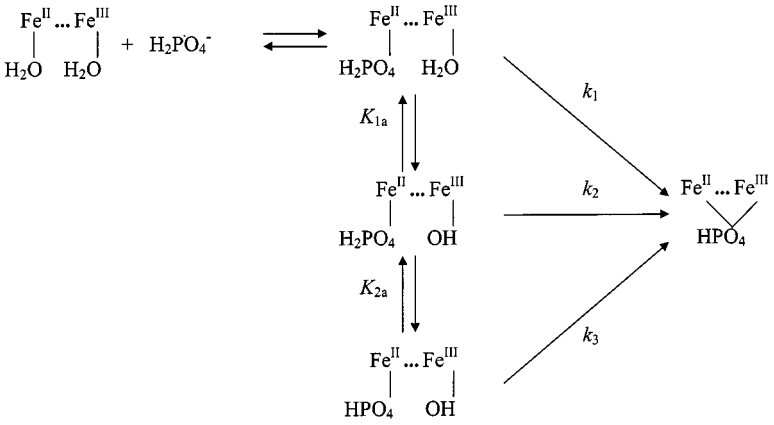

Scheme 1

Table 1. Summary of data obtained for the reactions (25°C) of $H_2PO_4^-$, phenylphosphate, pyrophosphate with active $Fe^{II}Fe^{III}$ PAP (Uf) at pH 2.6−6.5, I = 0.10M (NaCl)[16]

	$H_2PO_4^-$	Phenylphosphate	Pyrophosphate
pK_{1a}[a]	3.9	3.4	3.8
pK_{2a}[a]	5.1	5.0	5.4
pK_{1a}[b]	4.0		
pK_{2a}[b]	5.3		
pK_a[c]	6.9	5.6	6.0
k_1/s^{-1}	7.1	8.4	4.7
k_2/s^{-1}	1.8	1.0	2.3
k_3/s^{-1}	0.4	<0.1	0.1

[a] Recomputed using Microcal Origin 5 fitting program. − [b] Data for $Zn^{II}Fe^{III}$ Uf. − [c] Range of pK_a values for $H_2PO_4^-$ 6.7−7.0.

4.9.[86] As yet no explanation for this different behaviour of Uf as compared to BS and KBPAP has been forthcoming, although as already noted the pK_a′s assigned to $Fe^{III}-H_2O$ acid dissociation are smaller (3.9) for Uf than for BSPAP and KBPAP (4.9).

The acid dissociation process pK_{1a} giving the conjugate-base $Fe^{III}-OH$ slows down the substitution of $H_2PO_4^-$ at the Fe^{III}, but has a quite different effect on ester hydrolysis.

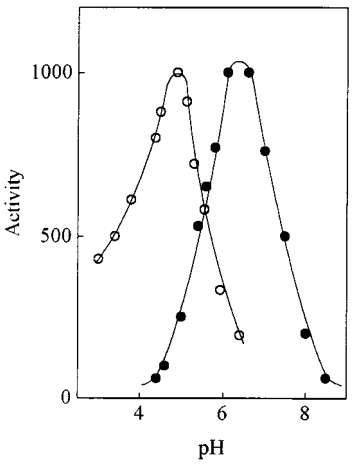

Figure 11. Variation of PAP phosphatase activity with pH, (a) for Uf (○) with 10 mM α-naphthyl phosphate (25°C) using 40 mM buffer;[16][80] and (b) for BSPAP (●), 50 mM *p*-nitrophenyl phosphate (22°C), using 100 mM buffer[100]

Phosphate Ester Hydrolysis

From the above considerations it is likely that the $Fe^{III}-OH$ conjugate-base induces phosphate ester hydrolysis. The suggestion that the μ-OH bridge might alternatively be involved,[87] seems less likely because of its less favourable nucleophilic properties. The $Fe^{III}-OH$ involvement is supported by the KBPAP catalysis of ^{18}O exchange between phosphate and solvent.[88] Rate constants k_{obs} for μ-phosphato formation are maximum at pH 3 when $Fe^{III}-H_2O$ is present exclusively. Under these conditions bridge closure can occur with displacement of the H_2O, but little or no phosphate ester hydrolysis is observed (Scheme 2). At higher pH formation and participation of $Fe^{III}-OH$ becomes more extensive, and k_{obs} decreases as the OH^- is more difficult to substitute than H_2O. However the $Fe^{III}-OH$ participates in ester hydrolysis by substitution into the P^V coordination sphere of $(RO)PO_3H^-$, with displacement of RO^- (Scheme 3). The activity plots as in Figure 11 now become relevant. The increase in activity of Uf at the lower pH′s is due to increased amounts of $Fe^{III}-OH$, which maximises at pH 4.9. The decrease in activity at the higher pH′s may relate to deprotonation of the positive patch histidines, making the binding of phosphate less effective.

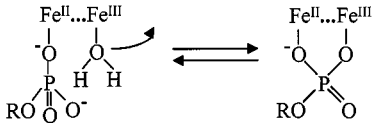

Scheme 2

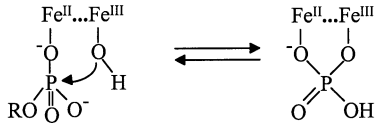

Scheme 3

The mechanism that emerges for PAP is thus one of repeated bridge formation and cleavage with ester hydrolysis taking place on a subsequent if not the first cycle. The reaction sequence has a number of features in common with the intramolecular phosphate hydrolysis occurring in the case of $[Co(en)_2(H_2O)\{PO_3(OC_6H_4NO_2)\}]^+$ (en = ethylenediamine), and involving the conjugate-base $[Co(en)_2(OH)\{PO_3\ (OC_6H_4NO_2\}]$.[89]

Metal Substituted PAP Derivatives

In order to clarify the role of individual metals as components of the dinuclear active site, the reactivity of metal substituted PAP′s has been studied. Work by Zerner and colleagues has shown that the Fe^{II} of active BSPAP is labile and amenable to substitution by various divalent metals (including Co^{II}, Cu^{II}, Zn^{II}, Cd^{II} and Hg^{II}).[41,76,83,90,91] The procedure used involves the reaction of PAP with dithionite for ≈ 5 minutes to remove the labile Fe^{II}, followed by reconstitution using an excess of the M^{II} salt. The effect of substitution of the Fe^{II} in Uf by Mn^{II}, Co^{II}, Ni^{II}, Cu^{II} and Zn^{II} on UV/Vis spectra and kinetic properties has been studied. In some cases (Figure 12) substantial catalytic activity is retained by the $M^{II}Fe^{III}$ product.

The Zn^{II} substituted form of Uf is of particular interest because it resembles the KBPAP active site (Figure 13). Previous studies have shown that the properties of the $Zn^{II}Fe^{III}$ form of the BSPAP enzyme are similar to those of KBPAP.[14,40,83] In a similar manner the Zn^{II} of KBPAP can be substituted by Fe^{II} to form a catalytically active $Fe^{II}Fe^{III}$. Again the properties of the $Fe^{II}Fe^{III}$ form of the KBPAP are similar to those of native $Fe^{II}Fe^{III}$ PAP forms,[92][93] and

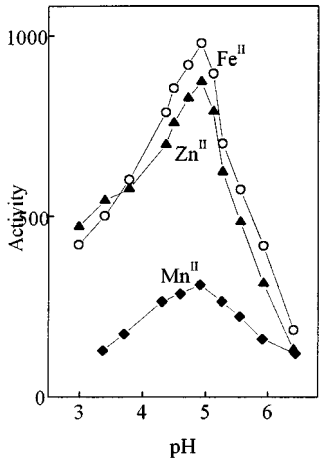

Figure 12. The variation of $M^{II}Fe^{III}$ Uf phosphatase activity (25°C) with pH (40 mM buffer) using α-naphthyl phosphate 10 mM), with M^{II} in turn Fe^{II} (○), Zn^{II} (▲), and Mn^{II} (◆)

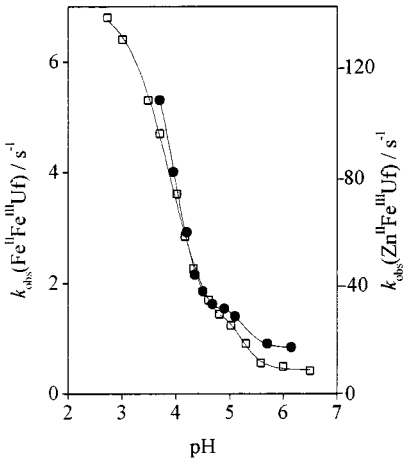

Figure 13 Variation of first-order rate constants k_{obs} (25°C) with pH for the reaction of $H_2PO_4^-$, with $Fe^{II}Fe^{III}$ Uf (□) and $Zn^{II}Fe^{III}$ Uf (●), I = 0.10M (NaCl)

vice versa for $Zn^{II}Fe^{III}$ Uf, although the reaction with $H_2PO_4^-$ is some 35 times more rapid than with $Fe^{II}Fe^{III}$ Uf at pH 4.9.[18] The $Mn^{II}Fe^{III}$ product is also of interest because Mn has been suggested as a component of sweet potato and soya bean PAP′s.[32,33,94–96] We note however that evidence for an $Fe^{II}Fe^{III}$ active site in sweet potatoes has also been reported.[97] It is unlikely that the active site contains $Mn^{II}Mn^{III}$ (as seems to be suggested), since Mn^{III}–Tyr charge transfer bands are not expected to give the same characteristic purple/pink colour as for Fe^{III} PAP′s. An appreciable blue-shift of ≈ 35 nm in phenolate to metal LMCT bands is for example observed for the Mn^{III} substituted transferrin (a lactoferrin form) as compared to the Fe^{III} form.[98]

From details of UV/Vis spectra (Table 2) it can be seen that the replacement of Fe^{II} with other divalent metals produces small but significant changes in peak positions (λ) and absorption coefficients (ε), where the products are different shades of purple. The greatest change in the peak position (λ) is for $Cu^{II}Fe^{III}$ Uf, and may indicate a different coordination of the Cu^{II}, which is known to have an affinity for *N*-donor ligands. The coupling of Fe^{II} to the Fe^{III},[45,50,51] appears to enhance ε values as compared to those for other M^{II} ions. The metal content and spectroscopic characterisation of PAP from sweet potato *Ipomea batatas* PAP has recently been carried out and establishes this as another example of a plant $Zn^{II}Fe^{III}$ protein.[99]

Table 2. UV/Vis peak positions (λ) and absorption coefficients (ε) for M^{II} substituted $M^{II}Fe^{III}$ PAP_r (Uf) (25°C), in sodium acetate buffer pH 4.9, I = 0.10M (NaCl)[80]

M^{II}	λ_{max}/nm	ε/M^{-1}cm^{-1}
Fe^{II}	510	4450[a]
Mn^{II}	514	3350
Co^{II}	518	3370
Ni^{II}	510	3260
Cu^{II}	545	3400
Zn^{II}	525	3580

Until recently metal substitution of M^{II} only was possible. In recent studies however the Fe^{III} centre has been replaced by Ga^{III} to produce $Fe^{II}Ga^{III}$ BSPAP and Zn^{II} Ga^{III} BSPAP.[100] Both forms exhibit catalytic activity similar to that of the native $Fe^{II}Fe^{III}$ BSPAP, providing evidence that diamagnetic Ga^{III} is acting as a functional analogue of Fe^{III}. Not surprisingly the gallium containing enzymes are colourless having lost the purple colour due to the tyrosine to Fe^{III} charge-transfer band. This work also provides kinetic data on the effect of substituting Fe^{II} with Zn^{II}. Thus the $Zn^{II}Fe^{III}$ BSPAP displays a 2–3 fold increase in K_M (the Michaelis constant), and nearly a twofold increase in k_{cat} relative to $Fe^{II}Fe^{III}$ BSPAP. The replacement of Fe^{II} and Fe^{III} of BSPAP to give $Zn^{II}Al^{III}$ and $Zn^{II}In^{III}$ has also been carried out.[101] There is as yet no explanation as to why the $Zn^{II}In^{III}$ form should be inactive.

Conclusions

The naturally occurring dinuclear $Fe^{II}Fe^{III}$ and $Zn^{II}Fe^{III}$ active sites of mammalian and plant purple acid phosphatases respectively make use of the M^{II} and Fe^{III} metal combination in a very subtle way to bring about phosphate ester hydrolysis. X-ray crystallographic studies on the enzyme from three different sources provides evidence for a single aqua or hydroxo ligand on each metal. The M^{II} ions are more labile, whereas Fe^{III} more readily forms conjugate-base (Fe^{III}–OH). The key roles are therefore binding of the phosphate ester to M^{II}, and the nucleophilic action of the OH^- of the Fe^{III} in bringing about phosphate ester hydrolysis. The $Fe^{III}Fe^{III}$ form of PAP has no similar enzymic action even though it does bind phosphate more strongly. The single tyrosine ligand serves to stabilise the Fe^{III} state and prevent its reduction. It also gives the enzyme its attractive colour. Other synthetic metal combinations can bring about phosphatase action although not always with the same efficiency. An essential part of the catalytic cycle is the release

of the μ-phosphate product after hydrolysis, a process which requires further investigation

[1] N. Sträter, W. N. Lipscomb, T. Klabunde, B. Krebs, *Angew. Chem. Int. Ed. Engl.* **1996**, *35*, 2024−2055.
[2] E. Wilcox *Chem. Rev.* **1996**, *96*, 2435−2458.
[3] J. B. Vincent, G. L. Olivier-Lilley, B. A. Averill, *Chem. Rev.* **1990**, *90*, 1447−1467.
[4] J. A. Stubbe, *J. Biol. Chem*. **1990**, *265*. 5329−5332.
[5] P. Nordlund, H. Eklund, *J. Mol. Biol*. **1993**, *232*, 123−164.
[6] J. D. Lipscomb, *Annu. Rev. Microbiol*. **1994**, *48*, 371−399.
[7] K. K Andersson, A. Graslund, *Adv. Inorg. Chem.*, **1995**, 43, 359−408.
[8] P. C. Wilkins, R. G. Wilkins, *Coord. Chem. Rev.* **1987**, *79*, 195−214.
[9] B. G. Fox, J. Shanklin, C. Somerville, E. Münck, *Proc. Natl. Acad. Sci., U. S. A.* **1993**, *90*, 2486−2490.
[10] N. Sträter, T. Klabunde, P. Tucker, H. Witzel, B. Krebs, *Science* **1995**, *268*, 1489−1492.
[11] T. Klabunde, N. Sträter, R. Fröhlich, H. Witzel, B. Krebs, *J. Mol. Biol*. **1996**, *259*, 737−748.
[12] J. B. Vincent, B. A. Averill, *FASEB J.* **1990**, *4*, 3009−3014.
[13] T. Klabunde, B. Krebs, *Structure and Bonding* **1997**, *89*, 177−198.
[14] J. L. Beck, L. A. McConachie, A. C. Summers, W. N. Arnold, J. De Jersey, B. Zerner, *Biochim. Bophys. Acta* **1986**, *869*, 61−68.
[15] M. A. S. Aquino, J.-S. Lim, A. G. Sykes, *J. Chem. Soc., Dalton. Trans.* **1992**, *13*, 2135−2136.
[16] M. A. S. Aquino, J.-S. Lim, A. G. Sykes, *J. Chem. Soc., Dalton. Trans.* **1994**, *15*, 429−436.
[17] M. A. S. Aquino, A. G. Sykes, *J. Chem. Soc., Dalton. Trans.* **1994**, *15*, 683−687.
[18] J.-S. Lim, M. A. S. Aquino, A. G. Sykes, *Inorg. Chem*. **1996**, *35*, 614−618.
[19] T. T. Chen, F. W. Baser, J. J. Cetorelli, W. E. Pollard, R. M. Roberts, *J. Biol. Chem*. **1973**, *248*, 8560−8566.
[20] H. D. Campbell, B. Zerner, *Biochem. Biophys. Res. Commun*. **1973**, *54*, 1498−1 1502.
[21] B. S. Allen, P. R. Nuttleman, C. M. Ketcham, R. M. Roberts, *J. Bone Miner. Res.* **1989**, *4*, 47−50.
[22] T. Efstratiadis, D. W. Moss, *Enzyme* **1985**, *33*, 34−40.
[23] K.-H. W. Lau, T. K. Freeman, D. J. Baylink, *J. Biol. Chem*. **1987**, *262*, 1389−1397.
[24] J. L. Beck, L. A. McConachie, A. C. Summers, W. N. Arnold, J. De Jersey, B. Zerner, *Biochim. Bophys. Acta* **1986**, *869*, 61−68.
[25] S. Fujimoto, T. Nakagawa, A. Ohara, *Agric. Biol. Chem.* **1977**, *41*, 599−600.
[26] K. Uehara, S. Fujimoto, T. Taniguchi, *J. Biochem.* **1974**, *75*, 627−628.
[27] S. Fujimoto, T. Nakagawa, S. Ishimitsu, A. Ohara, *Chem. Pharm. Bul*. **1977**, *25*, 1459−1464.
[28] A. H. J. Ullah, E. M. Mullaney, H. C. Dischinger Jr, *Biochem. Biophy. Res. Commun*. **1994**, *203*, 182−189.
[29] M. M. Jacobs, J. F. Nyc, D. M. Brown, *J. Biol. Chem*. **1971**, *246*, 1419−1425.
[30] C. Y. Li, L. T. Lam, *J. Histochem. Cytochem*. **1970**, *18*, 473−475.
[31] C. M. Ketcham, R. M. Roberts, R. C. M. Simmen, H. S. Nick, *J. Biol. Chem*. **1989**, *264*, 557−563.
[32] C. M. Roberts, G. A. Baumbach, F. W. Bazer, R. M. Roberts, *J. Biol. Chem*. **1985**, *260*, 5768−5776.
[33] J. Schinddelmeiser, D. Münstermann, H. Witzel, *Histochemistry* **1987**, *87*, 13−19.
[34] A. R. Hayman, T. M. Cox, *J. Biol. Chem*. **1994**, *269*, 1294−1300.
[35] B. Ek-Rylander, M. Flores, M. Wendel, D. Heinegård, G. Andersson, *J. Biol. Chem*. **1994**, *269*, 14853−14856.
[36] S. Shimohara, S. Fujimoto, M. Chachin, T. Taniguchi, G. Perry, P. J. Whitehouse, J. Kimura, *Brain Research* **1995**, *699*, 125−129.
[37] K. S. Patel, S. W. Lockless, B. Thomas, T. D. McKnight, *Plant Physiology* **1996**, *111*, 271.
[38] J. W. Pyrz, J. T. Sage, D. G. Debrunner, L. Que Jr, *J. Biol. Chem*. **1986**, *261*, 11015−11020.
[39] R. G. Wilkins, *Chem. Soc. Rev.* **1992**, *21*, 171−178.
[40] J. C. Davis, B. A. Averill, *Proc. Natl. Acad. Sci., U. S. A*. **1982**, *79*, 4623−4627.
[41] J. L. Beck, D. T. Keough, J. De Jersey, B. Zerner, *Biochim. Biophys. Acta*. **1984**, *791*, 357−363.
[42] D. F. Hunt, J. R. Yates III, J. Shabanowitx, N.-Z. Zhu, T. Zirino, B. A. Averill, S. T. Daurat-Larroque, J. G. Shewale, R. M. Roberts, K. Brew, *BioChem. Biophys. Res. Commun*. **1987**, *144*, 1154−1160.
[43] D. K. Lord, N. C. P. Cross, M. A. Bevilacque, S. H. Rider, P. A. Gorman, A. V. Groves, D. W. Moss, D. Sheer, T. M. Cox, *Eur. J. Biochem*. **1990**, *189*, 287−293.
[44] B. Ek-Rylander, P. Bill, M. Norgård, S. Nilsson, G. Andersson, *J. Biol. Chem*. **1991**, *266*, 24684−24689.
[45] A. I. Cassady, A. G. King, N. C. P. Cross, D. A. Hume, *Gene* **1993**, *130*, 201−207.
[46] T. Klabunde, B. Stahl, H. Suerbaum, S. Hahner, M. Karas, F. Hillenkamp, B. Krebs, H. Witzel, *Eur. J. Biochem*. **1994**, *226*, 369−375.
[47] T Klabunde, N. Sträter, B. Krebs, H. Witzel, *FEBS Lett*. **1995**, *267*, 56−60.
[48] M. Dietrich, D. Münstermann, H. Suerbaum, H. Witzel, *Eur. J. Biochem*. **1991**, *199*, 105−113.
[49] M. Merkx, B. A. Averill, *Biochemistry* **1998**, *37*, 11223−11231.
[50] B. A. Averill, J. C. Davis, S. Burman, T. Zirino, J. Sanders-Loehr, T. M. Loehr, J. T. Sage, P. G. Debrunner, *J. Am. Chem. Soc*. **1987**, *109*, 3760−3767.
[51] R. B. Lauffer, B. C. Antanaitis, P. Aisen, L. Que Jr., *J. Biol. Chem*. **1983**, *258*, 14212−14218.
[52] E. Sinn, C. J. O′Connor, J. De Jersey, B. Zerner, *Inorg. Chim. Acta*. **1983**, *78*, L13-L15.
[53] A. E. True, R. C. Scarrow, C. R. Randall, R. C. Holz, L. Que Jr., *J. Am. Chem. Soc*. **1993**, *115*, 4246−4255.
[54] Y.-S. Yang, J. M. McCormick, E. I. Solomon, *J. Am. Chem. Soc*. **1997**, *119*, 11832−11842.
[55] B. C. Antanaitis, P. Aisen, H. R. Lilienthal, *J. Biol. Chem*. **1983**, *4258*, 3166−3172.
[56] P. G. DeBrunner, M. P. Hendrich, J. De Jersey, D. T. Keough, J. T. Sage, B. Zerner, *Biochim. Biophys. Acta*. **1983**, *745*, 103−106.
[57] K. Doi, J. McCracken, J. Peisach, P. Aisen, *J. Biol. Chem*. **1988**, *26*, 5757−5763.
[58] B. C. Antanaitis, P. Aisen, *J. Biol. Chem*. **1985**, *260*, 751−756.
[59] D. L. Wang, R. C. H. Holz, S. S. David, L. Que Jr., M. T. Stankovich, *Biochemistry* **1991**, *30*, 8187−8194.
[60] B. C. Antanaitis, T. Strekas, P. Aisen, *J. Biol. Chem*. **1982**, *257*, 3766−3770.
[61] R. C Scarrow, J. W. Pyrz, L. Que Jr., *J. Am. Chem. Soc*. **1990**, *112*, 657−665.
[62] Z. Wang, L.-J. Ming, L. Que Jr., J. B. Vincent, M. W. Crowder, B. A. Averill, *Biochemistry* **1992**, *31*, 5263−5268.
[63] B. P. Gaber, J. P. Sheridan, F. W. Bazer, R. M. Roberts, *J. Biol. Chem*. **1979**, *254*, 8340−8342.
[64] S. A. Kretchmar, Z. E. Reyes, K. N. Raymond, *Biochim. Biophys. Res. Commun.* **1988**, *108*, 1643−1648.
[65] B. C. Antanaitis, J. Peisach, W. B. Mims, P. Aisen, *J. Biol. Chem.* **1985**, *260*, 4572−4574.
[66] J. T. Sage, Y.-M. Xia P. G. Debrunner, D. T. Keough, J. De Jersey, B. Zerner, *J. Am. Chem. Soc*. **1989**, *111*, 7239−7247.
[67] J. H. Rodriguez, H. N. Ok, Y.-M. Xia, P. G. Debrummer, B. E. Hinrichs, T. Meyer, N. H. Packard, *J. Phys. Chem*. **1996**, *100*, 6849−6862.
[68] L. W. Guddat, A. S. McAlpine, D. Hume, S. Hamilton, J. de Jersey, J. L. Martin, *Structure* **1999**, *7*, 757−767.
[69] J. Uppenberg, F. Lindqvist, C. Svensson, B. Ek-Rylander, G. Andersson, *J. Mol. Biol.* **1999**, *290*, 201−211.
[70] J. P. Griffith, J. L. Kim, E. E. Kim, M. D. Sintchak, J. A. Thomson, M. J. Fitzgibbon, M. A. Fleming, P. R. Caron, K. Hsiao, M. A. Navia, *Cell* **1995**, *82*, 507−522.
[71] C. R. Kissinger, H. E. Parge, D. R. Knighton, C. T. Lewis, L. A. Pelletier, A. Tempcyzk, V. J. Kalish, K. D. Tucker, R. E. Showalter, E. W. Moomaw, L. N. Gastinel, N. Habuka, X. Chen, F. Maldonado, J. E. Baker, R. Bacquet, J. E. Villafranca, *Nature* **1995**, *378*, 641−644.
[72] J. Goldberg, H.-B. Huang, Y.-G. Kwon, P. Greengard, A. C. Nairn, J. Kuriyan, *Nature* **1995**, *376*, 745−753.
[73] M. P. Egloff, P. T. W. Cohen, P. Reinemer, D. Barford, *J. Mol. Biol*. **1995**, *254*, 942−959.
[74] J. E. Coleman, *Annu. Rev. Biophys. Biomol. Struct.* **1992**, *21*, 441−483.

[75] E. G. Mueller, M. W. Crowder, B. A. Averill, J. R. Knowles, *J. Am. Chem. Soc*. **1993**, *115*, 2974−2975.
[76] R. C. Holz, L. Que Jr., L.-J. Ming, *J. Am. Chem. Soc*. **1992**, *119*, 4434−4436.
[77] X. Wang, L. Que Jr., *Biochemistry* **1998**, *37*, 7813−7821.
[78] T. W. Swaddle, A. E. Merbach, *Inorg. Chem*. **1981**, *20*, 4212−4216.
[79] See, for example, R. G. Wilkins in *Kinetics and Mechanism of Reactions of Transition Metal Complexes*, VCH, Weinheim, **1991**.
[80] M. B. Twitchett, A. G. Sykes, unpublished work.
[81] D. T. Keough, J. L. Beck, J. De Jersey, B. Zerner, *Biochem. Biophys. Res. Commun*. **1982**, *108*, 1643−1648.
[82] K. Doi, R. Gupta, P. Aisen, *J. Biol. Chem*. **1987**, *262*, 6982−6985.
[83] S. S. David, L. Que Jr., *J. Am. Chem. Soc*. **1990**, *112*, 6455−6463.
[84] S. K. Chapman, J. D. Sinclair-Day, A. G. Sykes, S.-C. Tam, R. J. P. Williams, *J. Chem. Soc., Chem. Commun.* **1983**, *20*, 1152−1154.
[85] C. F. Baes, E. Mesmer, *The Hydrolysis of Cations*, Wiley-Interscience, New York, **1976**.
[86] D. C. Schlosnagle, F. W. Bazer, J. C. M. Tsibris, R. M. Roberts, *J. Biol. Chem*. **1974**, *249*, 7574−7579.
[87] X. Wang, C. R. Randall, A. E. True, L. Que Jr., *Biochemistry* **1996**, *35*, 13946−13954.
[88] C. J. Wynne, S. E. Hamilton, D. A. Dianysius, J. L. Beck, J. De Jersey, *Arch. Biochem. Biophys.* **1995**, *319*, 133−141.
[89] P. Hendry, A. M. Sargeson, *Prog. Inorg. Chem*. **1990**, *38*, 201−258.
[90] D. L. Keough, D. A. Dionysius, J. De Jersey, B. Zerner, *Biochem. Biophys. Res. Commun*. **1980**, *94*, 600−605.
[91] J. L. Beck, M. J. McArthur, J. De Jersy, B. Zerner, *Inorg. Chim. Acta*. **1988**, *153*, 39−44.
[92] J. L. Beck, J. De Jersey, B. Zerner, M. P. Hendrich, P. G. Debrunner, *J. Am. Chem. Soc*. **1988**, *110*, 3317−3318.
[93] H. Sauerbaum, M. Körner, H. Witzel, E. Althaus, B.-D. Mosel W. Müller-Warmuth, *Eur. J. Biochem*. **1993**, *214*, 313−321.
[94] K. Uehara, S. Fugimoto, T. Taniguchi, *J. Biochem*. **1971**, *70*, 183−185.
[95] S. Fujimoto, A. Ohara, K. Uehara, *Agric. Biol. Chem*. **1980**, *44*, 1659−1660.
[96] S. Fujimoto, T. Nakagawa, A. Ohara, *Chem. Pharm. Bull*. **1977**, *425*, 3283−3288.
[97] S. K. Hefler, B. A. Averill, *Biochem. Biophys. Res. Commun*. **1987**, *146*, 1173−1177.
[98] R. M. C. Dawson, D. C. Elliott, W. H. Elliot, K. M. Jones, In *Data for Biochemical Research*, Oxford Sci. Pubs.
[99] A. Durmus, C. Eiken, B. H. Sift, A. Kratel, R. Kappl, J. Hüttermann, B. Krebs, *E. J. Biochem.* **1999**, *260*, 709−716.
[100] M. Merkx, B. A. Averill, Biochemistry **1998**, *37*, 8490−8497.
[101] M. Merkx, B. A. Averill, *J. Am. Chem. Soc* **1999**, *121*, 6683−6689.

Received February 9, 1999
[I99040]